Available online at www.sciencedirect.com
SCIENCE DIRECT®
Biochemical and Biophysical Research Communications 308 (2003) 165–169
BBRC
www.elsevier.com/locate/ybbrc

Surface trapping and AFM detection of DNA topological intermediates generated from an oxidative chemical nuclease☆

R. Mukhopadhyay,[a,*] S.G. Srivatsan,[b] and S. Verma[b,*]

[a] *Department of Biological Sciences and Bioengineering, Indian Institute of Technology Kanpur, Kanpur, Uttar Pradesh 208016, India*
[b] *Department of Chemistry, Indian Institute of Technology Kanpur, Kanpur, Uttar Pradesh 208016, India*

Received 20 June 2003

Abstract

Direct observation of DNA topological intermediates generated from a 'chemical nuclease' treatment has been made by atomic force microscopy (AFM). The intermediates were trapped at the mica–water interface and imaging was carried out in the dynamic force mode. Complete conversion from supercoiled circular state to relaxed circular/linear state has been observed over a time scale of 8 min. Implication of such studies in complementing gel electrophoresis data has been predicted.

Keywords: AFM; DNA; Oxidative cleavage; Chemical nuclease; Single molecule

Atomic force microscopy (AFM) has been applied to study the time-dependent function of a '*synthetic nuclease*' (9AA–Cu complex) on the conformational states of plasmid DNA pBR322. Observation of complete conversion of plasmid from its circular supercoiled to circular relaxed/linear state, over a time scale of 8 min, has been made and several topological intermediates were trapped and detected at the mica–water interface. To our knowledge, this is the first report of an AFM study on the effects of a non-biological nuclease on DNA topology.

Direct three-dimensional structural information on single biological molecules in their near native condition can be readily obtained from atomic force microscopic studies [1]. Relative ease of sample preparation and preservation of conformational features during AFM imaging, compared to transmission electron microscopy or cryo-electron microscopy, provides further impetus for using this technique to study biomolecular structural details. In addition to its use in studying DNA superstructures, applications of this method have been extended to study interactions of DNA with polylysine [2], RecA [3], restriction enzymes (*Pvu*II and *Hin*cII) [4], exonucleases [5], and cyanine dyes [6].

Phosphate ester (P-ester) modification induced by metal ion-containing adenylated polymeric templates has been reported earlier [7]. These constructs display Michaelis–Menten kinetics and behave as versatile heterogeneous catalysts. Modified adenine–copper redox couple relaxes the supercoiled DNA via oxidative route. It is surmised that the co-oxidant addition of magnesium monoperoxyphthalate (MMPP) possibly oxidizes Cu(II) to a hypervalent Cu(III)-oxo species, which results in the formation of either copper-bound non-diffusible radicals species or diffusible radicals [8]. These reactive species eventually lead to the DNA scission. The structural transformation of natural substrates like plasmid DNA by a simple adenine–copper catalyst (Fig. 1) acting as an oxidative chemical nuclease could be monitored by gel electrophoretic techniques as far as crude detection of circular supercoiled, circular relaxed, and linear forms is concerned. The need for detection and direct visualization of various topological intermediates with different structural characteristics at the

☆ *Abbreviations:* AFM, atomic force microscopy; DNA, deoxyribonucleic acid; MMPP, magnesium monoperoxyphthalate; P-ester, phosphate ester; AAC, acoustic alternating current; MAC, magnetic alternating current; APTES, aminopropyltriethoxysilane; EDTA, ethylenediaminetetraacetic acid; SPM, scanning probe microscopy; HPLC, high pressure liquid chromatography; 9AA–Cu, 9-allyl adenine–copper.

* Corresponding authors. Fax: +91-512-259-7103.
E-mail addresses: rupam@iitk.ac.in (R. Mukhopadhyay), sverma@iitk.ac.in (S. Verma).

0006-291X/$ - see front matter © 2003 Elsevier Inc. All rights reserved.
doi:10.1016/S0006-291X(03)01351-2

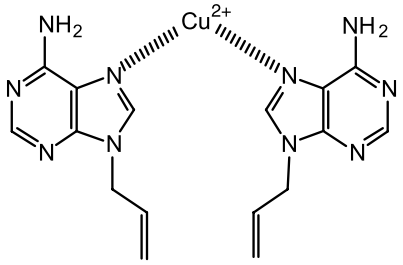

Fig. 1. 9-Allyl adenine–copper complex.

molecular level led to the present AFM study. A special interest was to explore the possibilities of the use of AFM as a complementary technique of gel electrophoresis. The present catalyst–DNA system was selected for no specific reason related to mechanism, but because both the components were previously characterized and therefore could be used as a model system.

Materials and methods

AFM setup, probes, and image acquisition. All the images were obtained using a Pico SPM equipment (Molecular Imaging) with an AFM A scanner. Images were obtained by the dynamic force mode. This mode involves cantilever oscillation either by an acoustic signal (AAC mode) [9] or by a magnetic signal (MAC mode) [10], leading to an enhanced resolution and minimal damage to the fragile biological samples. MAC mode was employed in all the experiments to circumvent the usual problem associated with AAC mode, i.e., masking of actual cantilever response by resonance from the cantilever holder and fluid body.

The fluid cell used for imaging under fluid was cleaned by keeping it in piranha solution (conc. sulfuric acid:hydrogen peroxide = 7:3 by volume) overnight and then washing and boiling in pure water for 15 min with occasional change of water. Imaging was performed immediately after cleaning the cell with freshly prepared sample under 100 μl HPLC grade water.

Au–Cr coated MAC cantilevers (Molecular Imaging), 85 μm long, and with a resonance frequency range of 22–25 kHz (in pure water) and force constant 0.06–0.1 N/m were used as obtained.

Scan speed was typically 1–2 lines/s. Minimum processing limited to 'first order flattening' and 'brightness contrast' was employed when necessary. The images are presented with inverted contrast for presentation purpose. Contour length was estimated by tracing the molecular contour with a segmented line.

Gel electrophoresis experiment. Plasmid cleavage reactions were performed in sodium cacodylate buffer (10 mM, 20 μl, pH 7.5, 30 °C), containing pBR322 supercoiled plasmid DNA (8 ng/μl), 9AA–Cu complex (100 μM), and activating agent [MMPP (100 μM)]. Individual reactions were quenched by adding gel loading buffer (5 μl) containing EDTA (100 mM), loaded onto 0.7% agarose gel, containing ethidium bromide (1 μg/ml), and electrophoresed for 1 h (70 mA). The destained gels were imaged using Bio-Rad GelDoc 2000 interfaced with a PC.

Preparation of AP mica. Freshly cleaved muscovite mica (ICR & Sons Pvt., India) was kept in contact of an aqueous suspension of APTES (Lancaster, UK) (water:APTES = 10,000:1 by volume) for 1 min, then washed with 1 ml of HPLC grade water (s.d. fine-chem, India), and dried in dry N_2 gas flow. APTES is known to generate positively charged surface that is essential for immobilization of polyanionic DNA molecules. A brief modification time ensures mild modification of the mica surface. This helps in immobilizing the molecules only with minimum substrate effect on the solution conformation of DNA molecules. The AP mica pieces were stored (10–15 min) in a covered box until use.

Sample preparation with plasmid DNA. The sample was prepared by deposition of 10 μl of 1 ng/μl plasmid solution [prepared in sodium cacodylate buffer (10 mM, pH 7.5)] on AP mica for 10 min, then washed with 1 ml (4 × 250 μl) of HPLC grade water, and immediately imaged under water.

Sample preparation with catalyst treated plasmid DNA. The sample was prepared from 1 ng/μl DNA solution obtained after catalyst treatment of 8 μl of DNA solution (2 ng/μl) in sodium cacodylate buffer. Two microlitres of each of 9AA–Cu complex (100 μM) and magnesium monoperoxyphthalate (MMPP) (100 μM) was added to DNA solution and kept for 1/3/5/8 min. MMPP possibly oxidizes Cu(II) to a hypervalent Cu(III)-oxo species, which results in the formation of either copper-bound non-diffusible radical species or diffusible radicals [8], eventually leading to DNA strand scission. At the end of the reaction time periods, 4 μl of EDTA (400 mM) was added to arrest the reaction. Sample preparation for AFM imaging was performed in the same manner as for untreated DNA solution. Imaging was carried out under HPLC grade water immediately after sample preparation.

Results and discussion

In Fig. 2, the topological course of chemical nuclease action as monitored by gel electrophoresis experiment over short reaction time spans (1, 3, 5, and 8 min) is presented. It is evident from this diagram that major conversion takes place in 5 min time, while complete conversion takes place by 8 min time period. The characteristic AFM images of the individual molecules before catalyst treatment are shown in Fig. 3. Complex

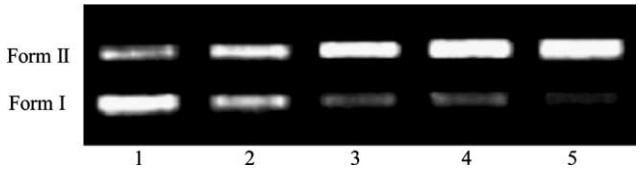

Fig. 2. Supercoiled plasmid DNA pBR322 cleavage by 9AA–Cu in the presence of MMPP. Lane 1, pBR322; lanes 2–5, pBR322 + complex + MMPP at 1, 3, 5, and 8 min reaction time. Form I: Supercoiled form and Form II: relaxed form.

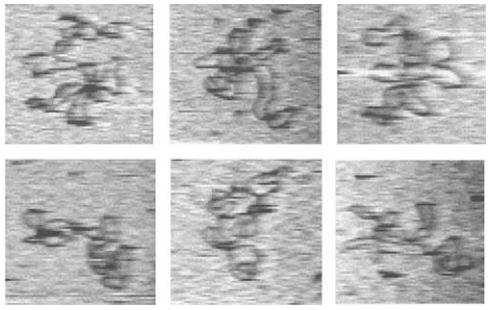

Fig. 3. Supercoiled plasmid DNA molecules before enzyme treatment (scan range: 250 × 250 nm).

tertiary structures with well-defined morphologies, for example, highly coiled structures (loop diameter in the range of 20–40 nm) with more than one crossover points are distinct in these images. Freshly cleaved mica, following surface modification by an aqueous suspension of aminopropyltriethoxysilane (APTES) [11] for a short period, was used for immobilization of the DNA molecules. Such treatment results in sparse positively charged mica surface that ensures optimal binding of the plasmid due to electrostatic interactions, while still maintaining its structural integrity. Continuous imaging over the same area did not cause any deformation in shapes and dimensions of the DNA molecules, reflecting minimum tip induced distortion and proper immobilization of the molecules on APTES treated mica (AP mica). Imaged width of the DNA molecules is determined to be 12 ± 3 nm, while the width known from X-ray studies is 2 nm [12]. The width widening in the AFM images compared to X-ray structure is due to the convolution between sample features and tip structure/shape. However, this is not expected to affect the overall conformation and the structural features resulting from nuclease action. A range of $\sim$6 nm in width values is observed because of tip-sample convolution effect and a variation in it associated with different tips used during AFM experiments. Different tips were used since tip quality deterioration during fluid phase imaging and consequent tip replacement with a new one was a routine phenomenon. The structures obtained in the adsorbed state could be related to the solution state structures as also previously done [13], since the environment and adsorption induced structural changes were minimized by imaging under fluidic conditions and by using mildly charged substrate surface, respectively.

Some linear molecules were observed along with the supercoiled molecules in the DNA sample before catalyst treatment. This is reflected from the upper band in lane 1 in gel electrophoresis diagram (Fig. 2) as well. No circular relaxed state was detected by AFM at this stage indicating the upper band be primarily due to the linearized state. However, the number of linearized molecules observed was fewer compared to that of the supercoiled molecules and the images of coiled molecules are selectively chosen and presented in Fig. 3, since the aim of this work was to monitor conversion of circular supercoiled DNA to its circular relaxed/linear state.

The DNA molecules with relaxed morphologies after 8 min treatment with the catalyst are evident from the imaged shapes shown in Figs. 4 and 5. This time period allows for a more extensive cleavage leading to higher degree of conformational changes, resulting in the formation of both circular relaxed and linear products of variable lengths and shapes. In Fig. 4A, two circular relaxed molecules (shown by arrows) are observed, while

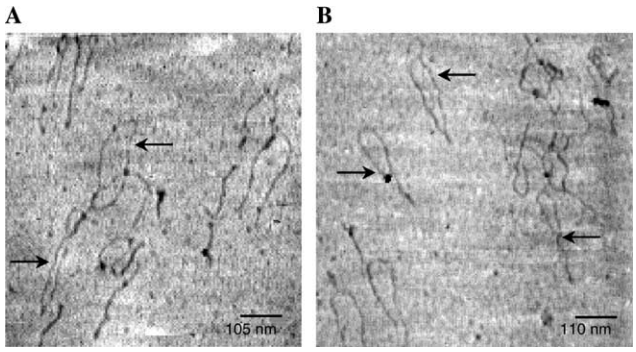

Fig. 4. (A) Two circular relaxed DNA molecules and linearized fragments and (B) several circular relaxed molecules are found scattered (after 8 min treatment).

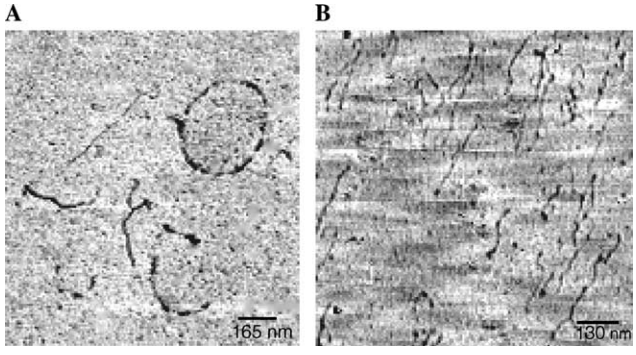

Fig. 5. (A) Smoothly bent circular DNA molecule along with linear fragments and (B) linear fragments (after 8 min treatment).

several such molecules are observed scattered in Fig. 4B. The loop diameter of these circular molecules along the short axis varies between 40 and 100 nm. In Fig. 5A, a smoothly bent circular molecule, with no observable superhelicity, is shown along with several linear fragments. The presence of both circular relaxed and linear DNA molecules (Figs. 4 and 5) indicates a strong possibility of single and double strand cleavage, respectively, of the plasmid [14]. A considerably greater number of linear molecules could be detected compared to the circular relaxed state indicating the upper band in lane 5 (Fig. 2) be primarily due to the linearized molecules.

Observation of linear molecules of different lengths (Figs. 4 and 5) indicates random multiple cleavage of the supercoiled plasmid leading to the smaller fragments. From a quantitative length distribution study (Fig. 6) on 40 linearized DNA fragments, it is observed that the average lengths lie in the range of 200–600 nm. No observation of fragments less than 100 nm or more than 1000 nm in length was made. This indicates insignificant cleavage from edges of the linearized molecule generated by initial cleavage of the plasmid. From Fig. 6, maximum cleavage appears to occur at the central region of the linearized plasmid.

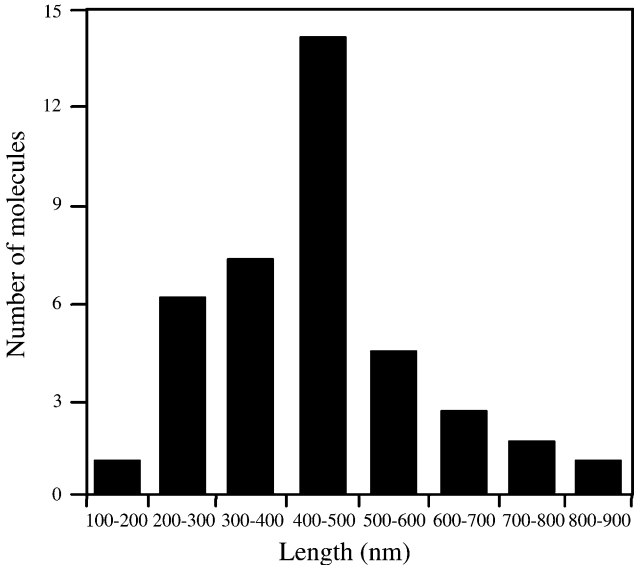

Fig. 6. Quantitative image analysis on the linear DNA fragments.

Catalyst treatment of the plasmid for 1, 3, and 5 min led to the observation of all the three topologies, i.e., circular supercoiled, circular relaxed, and linear, though for 5 min sample, it was primarily linearized molecules/fragments, some circular relaxed structures and rarely, coiled molecules (data not shown).

Control experiments were performed under water by imaging bare mica, AP mica, cacodylate buffer treated AP mica, AP mica treated with a solution of catalyst, co-oxidant, and EDTA in cacodylate buffer. No major contamination, surface roughening and DNA (coiled and relaxed) like features were observed. Plasmid treated with a solution of co-oxidant and EDTA was also imaged to look for any disruption of tertiary structure in the absence of the catalyst. No uncoiled and relaxed morphologies were detected and the structure of supercoiled plasmid molecules was observed intact.

In conclusion, direct evidence for relaxation of single supercoiled DNA molecules by oxidative chemical nuclease treatment has been obtained by AFM. We have shown that molecular level details can be obtained leading to more precise assignment of the bands in gel electrophoresis diagram, e.g., the upper bands in lanes 1 and 5 (Fig. 2) are primarily due to the linear state. Both the relaxed states, circular relaxed and linear, could be detected by AFM unlike gel electrophoresis and an idea about the cleavage characteristics (Fig. 6) could also be obtained. Very small amount of material (5–10 ng) is needed for an AFM study and importantly, the exact time for complete conversion from supercoiled to the circular relaxed/linear form can be obtained since a small number of coiled molecules can be detected by AFM, which is not possible in an ensemble experiment. It is evident that non-destructive surface trapping and AFM detection of nucleic acid topological intermediates can provide a powerful approach towards observation of a variety of structural modifications and therefore can complement corresponding studies performed with the conventional gel electrophoretic techniques.

Acknowledgments

R.M. thanks the Department of Biological Sciences and Bioengineering of Indian Institute of Technology Kanpur, for financial support, and Professors P. Sinha and A. Sharma for access to facilities. S.G.S. thanks Council of Scientific and Industrial Research (CSIR), Government of India, for a Senior Research Fellowship and S.V. thanks the Council of Science and Technology, UP, India, for financial support.

References

[1] (a) C. Bustamante, C. Rivetti, Visualizing protein–nucleic acid interactions on a large scale with the scanning force microscope, Annu. Rev. Biophys. Biomol. Struct. 25 (1996) 395–429;
(b) H.G. Hansma, Surface biology of DNA by atomic force microscopy, Annu. Rev. Phys. Chem. 52 (2001) 71–92.
[2] X. Shi, R.J. Sanedrin, F. Zhou, Structural characterization of multilayered DNA and polylysine composite films: influence of ionic strength of DNA solutions on the extent of DNA incorporation, J. Phys. Chem. B 106 (2002) 1173–1180.
[3] G.H. Seong, T. Niimi, Y. Yanagida, E. Kobatake, M. Aizawa, Single-molecular AFM probing of specific DNA sequencing using RecA-promoted homologous pairing and strand exchange, Anal. Chem. 72 (2000) 1288–1293.
[4] T. Nakamura, Y. Maeda, T. Oka, H. Tabata, M. Futai, T. Kawai, Atomic force microscope observation of plasmid deoxyribose nucleic acid with restriction enzyme, J. Vac. Sci. Technol. B 17 (1999) 288–293.
[5] K. Hori, T. Takahashi, T. Okada, The measurement of exonuclease activities by atomic force microscopy, Eur. Biophys. J. Biophys. Lett. 27 (1998) 63–68.
[6] J.A. Bordelon, K.J. Feierabend, S.A. Siddiqui, L.L. Wright, J.J. Petty, Viscometry and atomic force microscopy studies of the interactions of a dimeric cyanine dye with DNA, J. Phys. Chem. B 106 (2002) 4838–4843.
[7] (a) S.G. Srivatsan, M. Parvez, S. Verma, Modeling prebiotic catalysis with adenylated polymeric templates: crystal structure studies and kinetic characterization of template-assisted phosphate ester hydrolysis, Chem. Eur. J. 8 (2002) 5184–5191;
(b) S.G. Srivatsan, S. Verma, Nucleobase containing metallated polymeric resins as artificial phosphodiesterases: kinetics of hydrolysis, pH dependence and catalyst recycling, Chem. Eur. J. 7 (2001) 828–833;
(c) S.G. Srivatsan, S. Verma, Synthetic dephosphorylation reagents: rate enhancement of phosphate monoester hydrolysis by Cu(II)-metallated adenine nucleobase polymers, Chem. Commun. (2000) 515–516.
[8] C.J. Burrows, J.G. Muller, Oxidative nucleobase modifications leading to strand scission, Chem. Rev. 98 (1998) 1109–1151.
[9] P.K. Hansma, J.P. Cleveland, M. Radmacher, D.A. Walters, P.E. Hillner, M. Bezanilla, M. Fritz, D. Vie, H.G. Hansma, C.B. Prater, J. Massie, L. Fukunaga, J. Gurley, V. Elings, Tapping mode atomic force microscopy in liquids, Appl. Phys. Lett. 64 (1994) 1738–1740.

[10] W. Han, S.M. Lindsay, T. Jing, A magnetically driven oscillating probe microscope for operation in liquids, Appl. Phys. Lett. 69 (1996) 4111–4113.

[11] X.Z. Feng, R. Bash, P. Balagurumoorthy, D. Lohr, R.E. Harrington, S.M. Lindsay, Conformational transition in DNA on a cold surface, Nucleic Acids Res. 28 (2) (2000) 593–596.

[12] M.J. Allison, N.V. Hud, M. Balooch, R.J. Tench, W.J. Siekhaus, R. Balhorn, Tip-radius-induced artifacts in AFM images of protamine-complexed DNA fibers, Ultramicroscopy 42–44 (1992) 1095–1100.

[13] C. Pfannschmidt, J. Langowski, Superhelix organization by DNA curvature as measured through site-specific labeling, J. Mol. Biol. 275 (1998) 601–611.

[14] (a) A. Neves, H. Terenzi, R. Horner, A. Horn, B. Szpoganicz, J. Sugai, Hydrolytic DNA cleavage promoted by a dinuclear iron(III) complex, Inorg. Chem. Commun. 4 (2001) 388–389;
(b) T. Okubo, F. Nagai, K. Ushiyama, I. Kano, Contribution of oxygen radicals to DNA cleavage by quinone compounds derived from phenolic antioxidants, *tert*-butylhydroquinone and 2,5-di-*tert*-butylhydroquinone, Toxicol. Lett. 90 (1997) 11–18.